An *Ab Initio* Analysis of Charge Redistribution upon Isomerization of Retinal in Rhodopsin and Bacteriorhodopsin

BRITTANY CORN, SVETLANA A. MALINOVSKAYA

Department of Physics & Engineering Physics, Stevens Institute of Technology, Hoboken, NJ 07030

Received 31 December 2008; accepted 13 February 2009
Published online 30 April 2009 in Wiley InterScience (www.interscience.wiley.com).
DOI 10.1002/qua.22192

ABSTRACT: In the framework of quantum-chemical methods (RHF, MP2, and DFT), we study the reaction of photoinduced isomerization of biological molecules—retinal in rhodopsin (Rh) and bacteriorhodopsin (BRh)—the key intermediates in the vision process. The charge redistribution in the retinal chromophore of these biological molecules as the mechanism of the photoinduced isomerization is investigated. The results of the Mulliken, Löwdin, Natural Bond, and ESP population analyses are compared and validated. We demonstrate that the isomerization reaction is accompanied by the substantial charge relocation within the isomerization region with the electron localization on C11 for the retinal in Rh and C14 for the retinal in BRh. Int J Quantum Chem 109: 3131–3141, 2009

Key words: rhodopsin; charge distribution; isomerization; Löwdin population analysis

1. Introduction

Transduction of light detected by the eye into information is one of the most important biophysical processes. It is initiated by photon absorption and, through a series of photoinduced reactions, results in the stimulation of the optic nerve. Rhodopsin (Rh), a pigment produced in the rod cells of the retina, is well known for its primary role in the vision process. Isomerization of its retinal chromophore functions as a proton pump and is complete in only 200 fs, as proven through pump probe spectroscopy experiments by Shank et al. [1]. Resonance Raman Spectroscopy revealed that upon excitation of the Rh molecule by the absorbtion of light, 11-cis retinal twists about the C11=C12 bond, causing the tail end of the retinal molecule to flip into the trans position (Fig. 1) [2]. It has also been proposed by Lin et al. that this flip is due to the steric interaction between the methyl group of C13a and H10, the hydrogen attached to C10 [2]. However, an explanation for the mechanism of the drastic

Correspondence to: S. Malinovskaya; e-mail: smalinov@stevens.edu

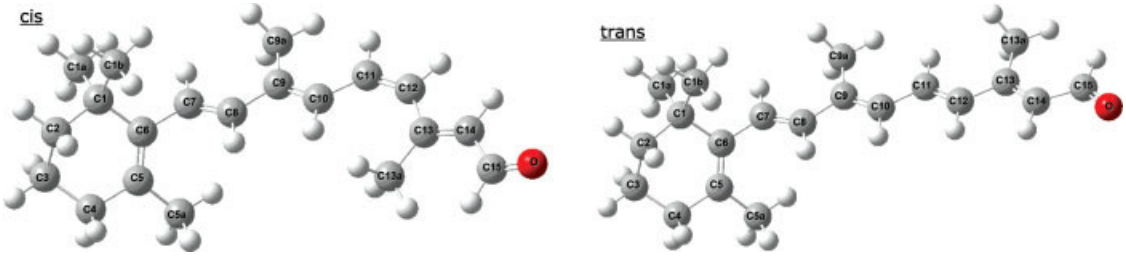

FIGURE 1. The 11-cis and all-trans retinal configuration of rhodopsin optimized with RHF/6-31++G**. [Color figure can be viewed in the online issue, which is available at www.interscience.wiley.com.]

change in structure of retinal during this process is still unclear.

Recent terahertz studies by Groma et al. observed a large induced polarization effect that occurs due to ultrafast electron transfer inside the retinal chromophore upon the excitation of bacteriorhodopsin (BRh) [3], an analogue of Rh found in archaea, single-celled microorganisms. Upon absorption of the pulse, a dipole moment is induced in the BRh molecule, generating an electric field, which, when coherently summed over the entire sample, produces a terahertz signal. We deduce that the electric field induced in the retinal chromophore upon excitation interacts with the charged particles of the molecule, therefore, inducing the dynamical changes inherent to the isomerization. To quantify the change in atomic charge throughout the molecule, we compared the population analyses of the initial, 11-cis, and final, all-trans, retinal configurations. Based on this charge distribution analysis and our knowledge of the reaction path from spectroscopic data [4], we propose charge transfer as the mechanism behind the isomerization. Calculation of the transition state would further prove our hypothesis, however, is beyond the scope of this article. All numerical calculations were performed with the computational package Gaussian03 [5].

The charge distribution of a molecule is useful for various purposes, such as calculating multipole moments and other electrostatic properties. It is often necessary to rely on numerical calculations using quantum-chemical methods to perform the population analysis of molecules. However useful, the reliability of these methods is variable depending on the method of optimization, basis set, and type of population analysis used. Testing the accuracy of the charge distribution is a study of its own. One can make a wide-ranged comparison over the factors mentioned above and measure them up to experimentally observed values, as was done by Martin et al. for the water molecule [6]. The task becomes more challenging when we introduce a molecule like retinal in Rh that has increasing complexity and is lacking data to match up to it.

To add another degree of comparison in our investigations, we performed the charge distribution analysis for 13-cis retinal, Figure 2, the chromophore present in Bacteriorhodopsin (BRh). Interestingly, the retinal in BRh is identical in structure to that of Rh, however, it experiences an all-trans to 13-cis isomerization about the C13=C14 double bond. The fact that this retinal molecule undergoes the same mechanism in the opposite direction about an adjacent bond can bring interesting insight in comparison to the charge dynamics that occur during the isomerization of Rh.

A point of interest is optical control of the isomerization in Rh and BRh. Recent experiments by Prokhorenko et al. involving pulse shaping techniques showed the ability to enhance the isomerization yield by up to 20% [7], a great addition to the naturally ≈60% efficient process [8]. Bringing understanding to the mechanism of the isomerization can provide insight into the coherent control of the reaction.

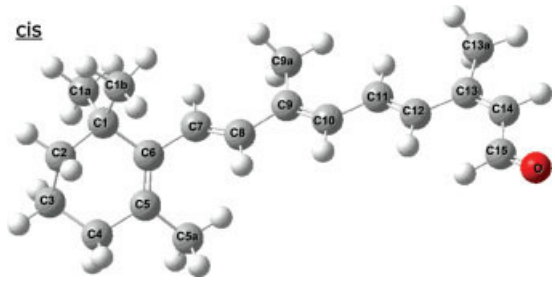

FIGURE 2. 13-cis retinal configuration optimized using RHF/6-31++G** (bacteriorhodopsin). [Color figure can be viewed in the online issue, which is available at www.interscience.wiley.com.]

TABLE I

The ground-state energy of 11-cis retinal in rhodopsin calculated by RHF, MP2, and DFT methods using twelve basis sets.

	STO-3G	3-21G	6-31G	6-311G
SCF Energies in a.u.				
RHF	−838.1626	−843.7340	−848.1145	−848.2710
MP2	−839.3531	−845.6660	−850.0521	−850.3464
DFT/B3LYP	−843.6820	−849.4867	−853.9445	−854.1294

Polarization functions		Diffuse functions		Polarization and diffuse fns.	
RHF optimization energies in a.u.					
3-21G	−843.7340	6-31G	−848.1145	6-31G	−848.1145
3-21G*	−843.7340	6-31+G	−848.1312	6-31+G**	−848.5147
3-21G**	−843.8772	6-31++G	−848.1320	6-31++G**	−848.5154

In the following section, we will present our basis set of choice and optimization methods used for the retinal molecule. In section 3, we will discuss the population analyses (Mulliken, Löwdin, natural, and electrostatic potential) and compare them between ab initio and density functional optimization methods (RHF, RMP2, DFT/RB3LYP) for 11-cis and all-trans retinal in Rh as well as 13-cis retinal of BRh. We will discuss the physical interpretation for each population analysis. Last, we will assert which population method is most accurate for larger molecules and also draw conclusions about the charge relocation in the retinal molecule upon the isomerization of Rh.

2. Optimization Method and Basis Set

There are many factors that go into selecting the correct optimization method and basis set for a molecule. Inspection of the atomic structure of the molecule, which in this case contains 20 carbon atoms, 28 hydrogen atoms, and one oxygen atom, indicates that restricted, or closed shell, methods are to be used due to an even number of electrons. To find the most favorable configuration for use in the population analysis calculations, we performed an optimization of 11-cis retinal in the framework of three methods (Hartree–Fock, MP2, and DFT with a B3LYP functional) and four basis sets (STO3-G, 3-21G, 6-31G, and 6-311G [9, 10]) shown in Table I. The detailed results of the implemented methods will be given in the next section.

According to Hartree–Fock theory, the increase of the basis set is known to cause the optimized SCF energy to approach the Hartree limit [9]. As shown in Table I, as the size of the basis set is increased within the HF method, the optimized SCF energy becomes lower and lower, referring to a more stable configuration of the molecule. By also taking computational time into consideration, we chose the 6-31G basis set.

Next, we evaluated the need for polarization and diffuse functions. Adding polarization functions to the basis set allows for more flexibility in the presence of hybrid orbitals [10]. As shown in Table I, adding polarization functions to only the heavier atoms, that is, carbon and oxygen, had no effect, whereas adding them to both the heavier and lighter atoms, now including hydrogen, lowered the ground state equilibrium energy. These results show that the polarization functions allowed for a better representation of the sp^3 orbitals of the carbon atoms in the methyl groups, and the sp^2 orbitals of the carbon atoms along the chain.

We also analyzed the option for adding diffuse functions to the basis set. These are shallow Gaussian functions that when added to the minimal basis set, allow for a better representation of the tail end of certain orbitals [10]. Calculations showed that adding diffuse functions to the heavier atoms and to both the heavy and light atoms both gave a lower ground state energy. Therefore, for retinal, the 6-31++G** basis set is the most appropriate choice.

Now that the most fitting basis set has been chosen, we can explore deeper into the optimization methods. We made a full geometry optimization of

TABLE II

The ground-state energy difference for the 11-cis and all-trans configurations calculated using RHF, MP2, and DFT/B3LYP methods when compared with the experimental value.

Method	Energy gap (eV)
RHF	0.257
MP2	0.190
DFT/B3LYP	0.218
Experiment [7]	0.206

the 11-cis and all-trans retinal configurations using the RHF/6-31++G** method, the DFT method with RB3LYP/6-31++G**, and the RMP2/6-31G method followed by a single point RMP2/6-31++G** calculation. The energy gap in going from cis to trans is shown in Table II. The magnitude of the energy difference, for all three methods, matches the known experimental value 0.206 eV [8, 11] quite well. It is valuable to compare population analyses amongst all three optimization methods.

3. Population Analyses

There are numerous population analyses available, each with a different advantage point [9, 10, 12, 13]. In general, a population analysis calculates the expected amount of charge one would find on each atom of the molecule. The complexity of the problem becomes obvious when referring to a covalent bond between a pair of atoms in the retinal chromophore. Depending on the bond length and the type of atoms involved, one can then assign an amount of partial charge to each atom based on the probability of that electron being present near the atom. How one allocates the partial charge is determined by the type of population analysis used.

The first method we focus on is the Mulliken Population Analysis, which is most commonly known for its ease of calculation. On the other hand, it tends to oversimplify the distribution of partial charge, especially for large and complex molecules. When it comes to an electron which is shared between atoms, referring to an off-diagonal element in the population matrix, Mulliken splits the partial charge evenly amongst the atoms involved [9]. The second type of method sets out to improve on the Mulliken Analysis. The Löwdin population analysis first orthonormalizes the set of basis functions, therefore, eliminating the need to redistribute the shared charge [9]. The natural population analysis (NPA) uses a similar tactic, however, sets out to preserve the shape of the atomic orbitals [9]. A third type of analysis is known as electrostatic potential, or ESP. In this method, the amount of partial charge allotted to each atom is made to fit the pre-calculated electrostatic potential of the molecule [12]. Merz-Kollman (MK) chooses points around the molecule to calculate the potential at a density of 1 point per Å, whereas CHELPG uses over ten times more points than MK. Using the above mentioned population methods, we have calculated the atomic charge distribution for both the 11-cis and all-trans retinal configurations. A change in the charge distribution of the initial and final structures correlates to the conformational changes in retinal that are observed experimentally [1, 4] and are well-known to the photoisomerization reaction. Therefore, we deduce that charge transfer occurs based on the results of the initial and final retinal structures. By taking the difference between the populations, we quantified how much the electron redistribution contributes to the mechanism of the isomerization of retinal in Rh.

The amount of partial charge on an atom is measured in the absolute value of the magnitude of an electron. Therefore, in the following charts, a negative value refers to electrons gained by the atom, and a positive amount, electrons lost. We take a closer look for the following three optimization methods.

3.1. HARTREE–FOCK

The Hartree-Fock method [10] is commonly used, mainly for its ease of calculation as well as successful results. Upon optimization of both 11-cis and all-trans retinal with the RHF method, it is interesting to note the differences in structure of the two configurations. Although there were no significant changes in bond lengths, there were many readjustments of linear and dihedral angles. Since the 11-cis retinal optimized structure has the tail leaning slightly into the plane, we assume that the dihedral twist about the C11=C12 double bond occurs counterclockwise by 177 degrees. The atoms immediately surrounding this bond adjusted in such a way to make the carbon backbone of the trans configuration appear planar (Fig. 1). In the trans configuration, the p orbitals along the carbon chain are lined up in a way to facilitate overlapping and, therefore, the redistribution of charge.

Evaluating the relocation of charge, we see a separation of the five methods into three types;

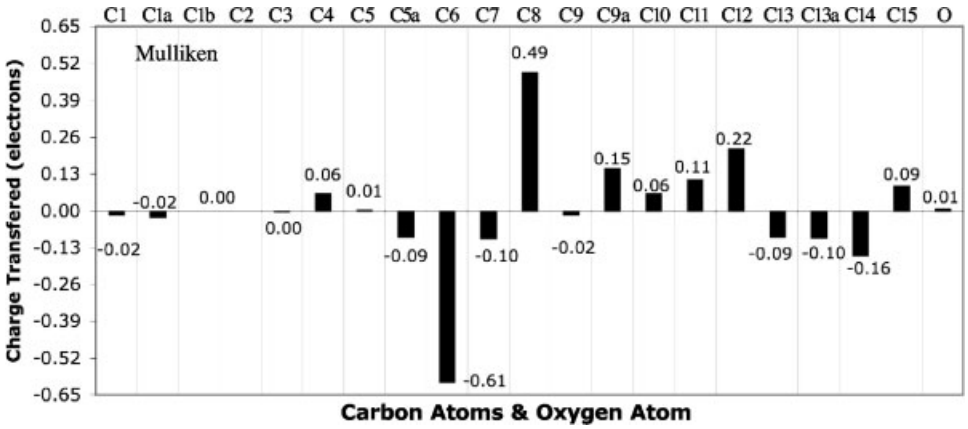

FIGURE 3. Charge transfer in rhodopsin calculated using the Mulliken population analysis with structures optimized by the RHF method.

the Mulliken analysis, the NPA and Löwdin analysis, and the electrostatic potential methods (MK and CHELPG). The Löwdin and NPA analyses give coherent results, due to their similarity of method. On the other hand, MK and CHELPG have a similar method except show qualitatively different results. This is evidence for their lack of consistency for such a complex molecule as retinal. The ESP methods are also known to be sensitive to slight changes of configuration [9], so testing charge redistribution in retinal upon isomerization would give erratic results.

At a closer look, each population analysis makes a different prediction for the charge relocation in 11-cis retinal upon isomerization of Rh. The Mulliken population analysis, shown in Figure 3, shows the largest amount of electrons gained by C6 and lost by C8. This is an unexpected result because there is no change in structure involving either of these atoms. However, it signifies a change in the molecular orbitals in this region. There also shows to be a lot of activity in the isomerization region. In this analysis, the charge from C9a to C12 travels toward the end of the molecule and localizes mostly at C14, which also gains negative charge from C15.

A more distinct relocation of charge occurs in the Löwdin population analysis, Figure 4(a). It is most apparent that the charge from the C10 carbon is distributed to its surrounding atoms, C9 and C11. This could be a manifestation of the steric interaction with the C13a methyl group [2], causing C10 to readjust so strongly. A similar effect occurs on the 12th carbon atom, which allocates charge to the 11th and 13th carbon atoms. One can imagine the repulsion between H10 and the C13a methyl group causing C10 to thrust charge away and facilitating the flip about the C11=C12 bond, which readjusts its orbitals to form a planar backbone.

Comparably, the natural population analysis (NPA), Figure 4(b), gives similar results. For this method, the only significant relocation of charge is the large loss by the 10th carbon atom which is then gained by the 9th and 11th carbon atoms. Because NPA tries to replicate the atomic orbitals present on the molecule, this is another hint toward the significant change in orbitals around the 10th carbon atom. This analysis strongly shows the role that C10 plays in the isomerization of Rh, as expected by Lin et al. [2].

The electrostatic potential-based population analyses gives very different results. The Merz-Kollman analysis, Figure 5(a), shows a somewhat even charge redistribution throughout the entire molecule. The largest relocation of charge occurs in two areas. One is the loss of negative charge by the 6th carbon atom, which is apportioned to all adjacent atoms, such as C1 and C5 in the β-Ionone ring, and mostly to C7. The other occurs on the opposite end of the molecule, on the 13th carbon atom. C13 gains charge from its surrounding atoms: C12, C13a, and C14. Another comparable amount of negative charge is gained by C10 from C11 and C9.

Last, the CHELPG analysis in Figure 5(b) shows entirely different results. This population analysis felt the largest effect on the methyl groups, where the largest amount of charge was gained by the carbon attached to the 13th carbon, labeled as C13a. This gain is correlated with the loss of electrons by C14. It is also worth mentioning that in all other population analyses, there was a negligible amount of charge

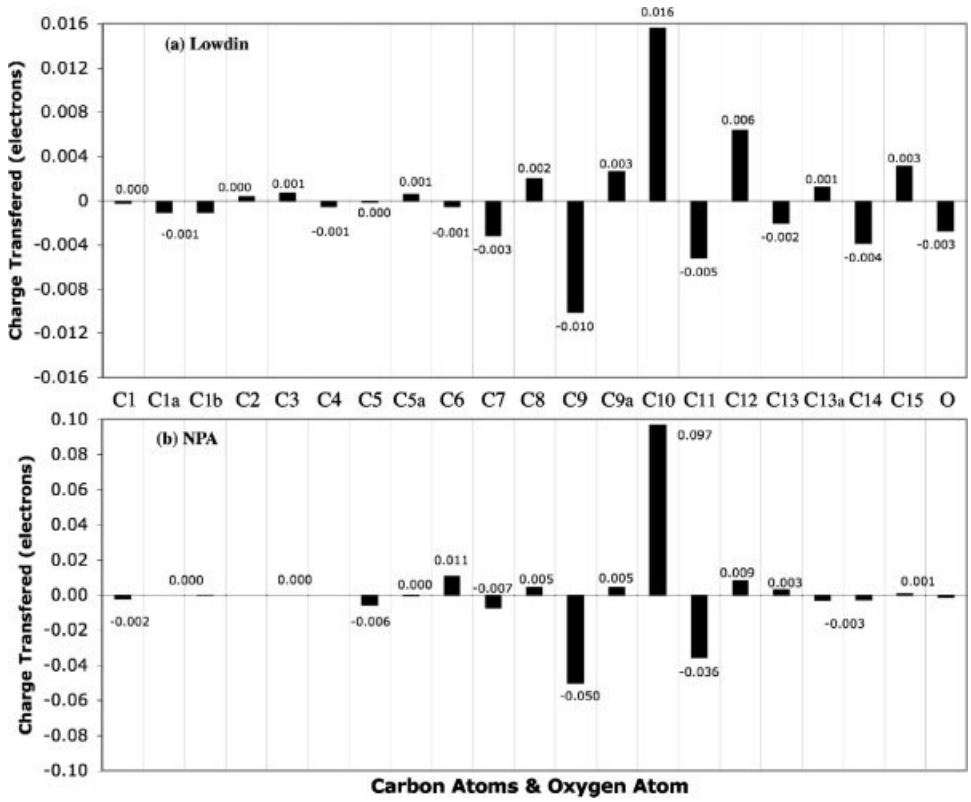

FIGURE 4. Charge transfer in rhodopsin calculated using the (a) Löwdin and (b) natural population analyses with structures optimized by the RHF method.

redistribution on the hydrogen atoms. In the case of CHELPG, however, a significant amount of charge is lost by one of the hydrogen attached to C13a. The next largest relocation of partial charge occurred around the 9th carbon atom. It redistributed its charge to C9a, C10, and a small amount to C8. The last significant amount of charge lost was by C1a and C5a, both carbons within the methyl groups attached to the β-Ionone ring, which spread their charge out to their attached hydrogens. Another observation is that there was no relocation of charge by the 11th and 12th carbon atoms at all. Therefore, the CHELPG analysis attributes the torsional flip of 11-cis retinal in the isomerization of Rh to interactions between all methyl groups with their surrounding atoms.

To validate the results discussed above, we analyzed the charge redistribution in going from all-trans to 13-cis retinal in BRh using the same five population methods. Because the isomerization occurs about the C13=C14 double bond, we expect to find a localization of charge in similar regions to that of Rh, however, migrating in the opposite direction. On the other hand, the isomerization of BRh does not exhibit the large movement of the C13a methyl group, as does Rh, so the affects of this steric interaction should not arise. The Löwdin and natural population analyses show to have an analogous representation of the charge dynamics for retinal between Rh and BRh, whereas the Mulliken and ESP analyses have no correlations between the two molecules.

We focus on the Löwdin population analysis for the charge relocation within 13-cis retinal upon isomerization of BRh in Figure 6(a). Here, we see the most activity by C11 which sends most of its charge to C12, as well as to C10. This is analogous to the Löwdin analysis of charge relocation in 11-cis retinal of Rh, which going oppositely from cis to trans, depicts C11 gaining charge from C10 and C12. The next observation is in the isomerization region where the analysis shows charge from C15 localizing on C14, an effect which also occurs in Rh. Next, it is apparent that the natural population analysis for the retinal in BRh is almost identical to the mirror image of that for Rh. The most prominent outcome is the large gain of negative charge by C10 from C11 and C9, the exact opposite of the cis-trans charge dynamics shown by the retinal in Rh. The NPA continues to

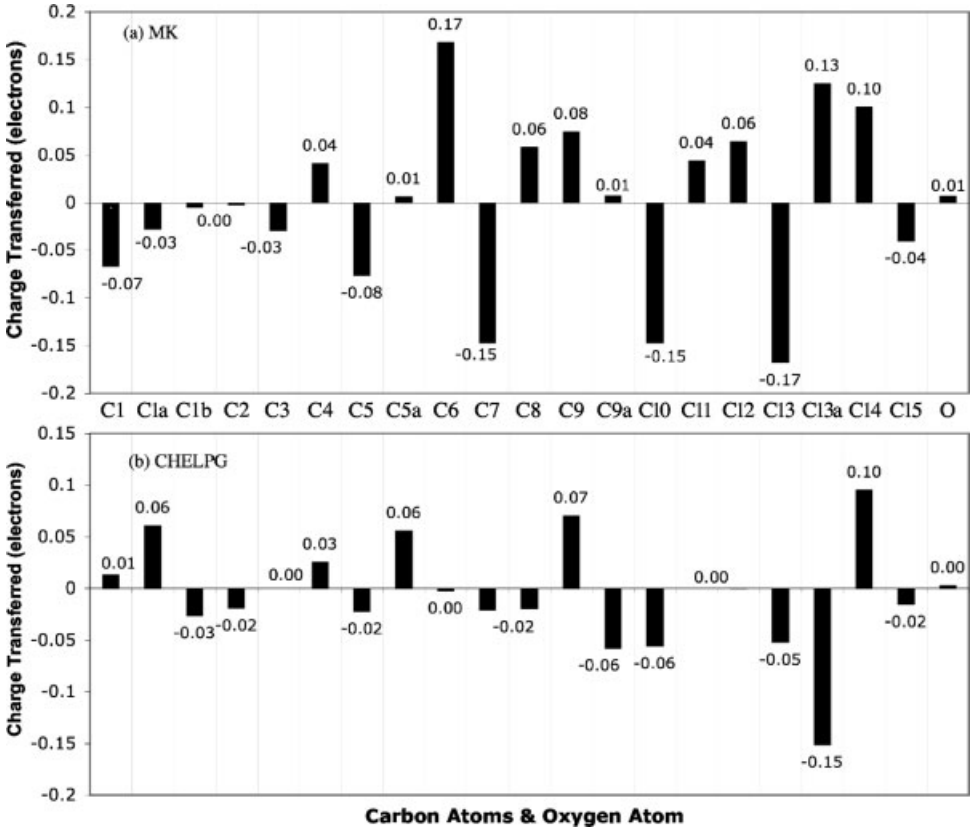

FIGURE 5. Charge transfer in rhodopsin calculated using the (a) Merz-Kollman and (b) CHELPG ESP population analyses with structures optimized by the RHF method.

give importance to the C10 redistribution of charge as a significant part of the isomerization mechanism.

If we look specifically in the region of isomerization for the Löwdin population analysis and NPA, we find there is a comparable redistribution of charge for the two molecules. For the retinal in Rh, negative charge flows from C12 to C11 in going from the 11-cis to all-trans configurations. Conversely, for the trans to 13-cis isomerization of BRh, the charge flows from C13 to C14. We can draw the analogy between C12 of Rh and C14 in BRh and remark that they play similar roles in their respective isomerization mechanisms.

From the change in charge distributions of the retinal chromophore in Rh and BRh within the Hartree Fock method, it is evident that the Löwdin and natural population analyses are the most consistent under these criteria and provide the most relevant interpretation for charge redistribution. We can draw preliminary conclusions from these analyses and move on to validate them from the different perspectives of the MP2 and DFT optimization methods.

3.2. MP2 ANALYSIS

The second optimization method, we focus on is Moller–Plessent theory. As an improvement to HF theory, the electron–electron interactions are treated as a perturbation. By solving for the eigenvalues and eigenfunctions of the sum of single-electron Fock operators, our unperturbed Hamiltonian, we can then solve for the correction energies. Applying first order perturbation theory remarkably gives the Hartree-Fock energy, confirming that HF theory is a reliable theory on its own [9]. However, for the isomerization of Rh, electron interactions play an important role in the conformational changes of retinal, making it beneficial to include the electron correlation in a more exact way. We do so by applying second order perturbation theory, also known as MP2. Because of the time constraints, these population analyses were obtained by first optimizing the structure with the 6-31G basis set, then performing a single-point energy calculation with the 6-31++G** basis, an approach found in [6]. The

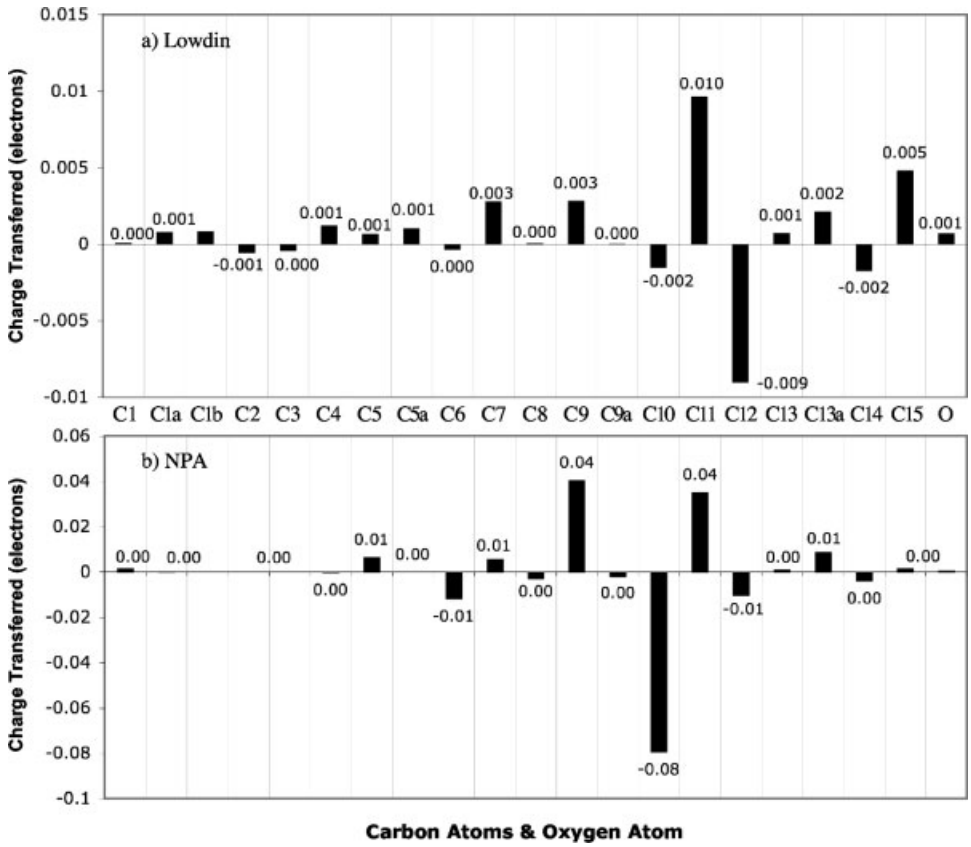

FIGURE 6. Charge transfer in bacteriorhodopsin calculated using the (a) Löwdin population analysis and (b) natural population analysis with structures optimized by the RHF method.

restricted MP2 method with the latter basis set provided a significantly lower equilibrium energy by almost 3 au.

By analyzing the MP2/6-31++G** 11-cis retinal structure and comparing it to that of the HF method, we observed the elongation of all bonds along the carbon backbone. This greater distance between atoms is due to the inclusion of electron correlation in the MP2 method which causes electron–electron repulsion effects as well as the separation of positively charged nuclei. The Löwdin and natural population analyses also highlight effects due to these interactions in Figure 7.

Immediately, one can notice the resemblance between the MP2 Löwdin charge redistribution results in Figure 7(a) and the HF results in Figure 4(a). Our attention is first drawn to the C10 carbon, which again drives its charge to the C9 and C11 atoms. Also present is the relocation of charge from C12 to C11 in the isomerization region. The MP2 calculation brings a new perspective to the charge redistribution analysis by revealing the loss of charge from C13a. This methyl-group carbon allocates a significant amount of charge to its attached hydrogen atoms. A gain of negative charge on the hydrogen would mean an increase in the repulsion between the methyl group and H10 atoms, therefore, driving the tail end of the retinal molecule to flip into the trans position.

The natural population analysis also reflects this description of the charge redistribution mechanism in the retinal of Rh, however, adds new effects as well. Turning to the isomerization region in Figure 7(b), we do not see the alternating redistribution of charge as in the Löwdin analysis [Figure 7(a)] but rather the loss of charge by all atoms between C9—C13. This implies that the hydrogen attached to the carbon atoms in this region play a more instrumental role in the charge redistribution mechanism. Most significant is the large gain of negative charge by H11, the hydrogen attached to C11, which receives the largest amount of charge out of the entire molecule. The next largest gain is by the H12 hydrogen connected to C12. Experimentally, a large decoupled wag mode was assigned to the H11 and H12 hydrogen-out-of-plane(HOOP) modes [1] which were later proposed by Yan et al. to be a

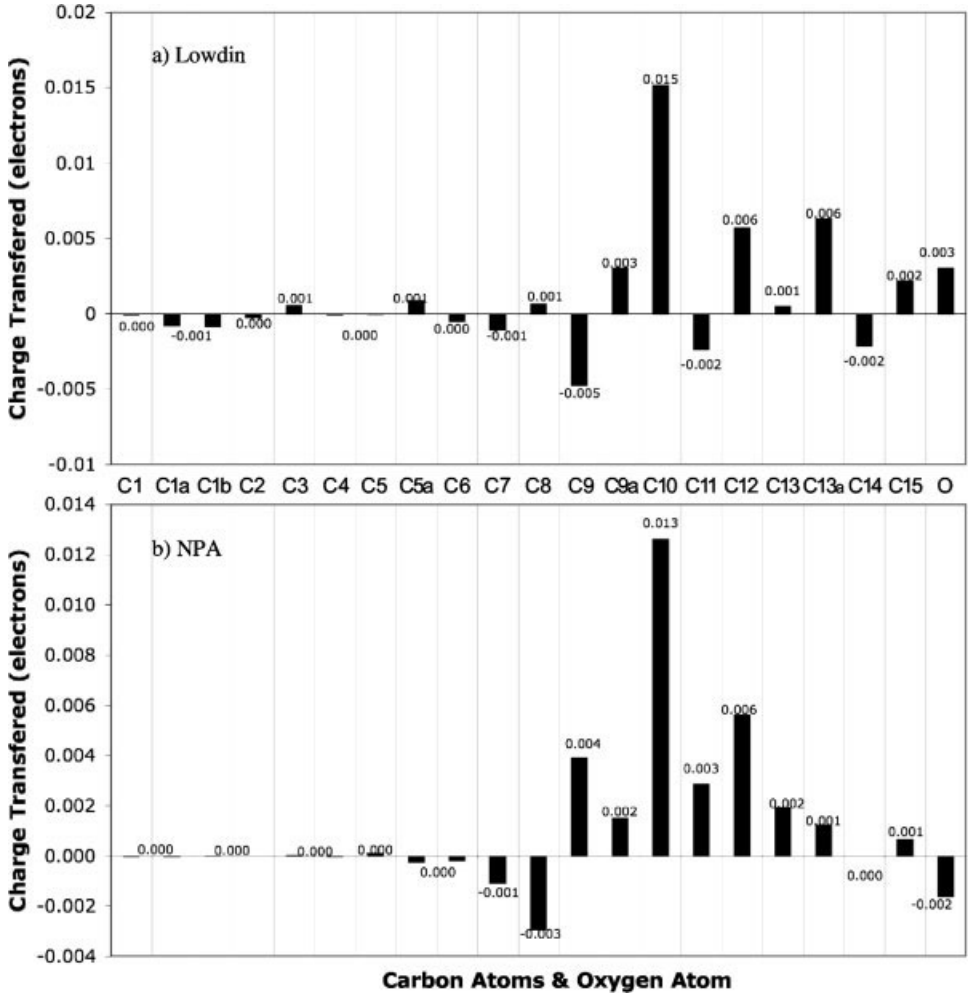

FIGURE 7. Charge transfer in rhodopsin calculated using the (a) Löwdin population analysis and (b) NPA with structures optimized by the MP2 method.

demonstration of the large twist about the C11=C12 bond [14]. Evidence is also shown in our calculations for the steric interaction [2] between the C13a methyl group and the H10 hydrogen through the large loss of charge by the C10 carbon as well as the large gain of negative charge by all of the hydrogens attached to C13a.

It is notable that by including the electron correlation effects through the MP2 method, both the Löwdin and natural population analyses emphasized many of the well-known effects that were experimentally observed for the isomerization of Rh [1–3, 14]. NPA, which sets out to reproduce the shape of the atomic orbitals of the molecule, included the presence of the HOOP mode hydrogens as playing a role in the isomerization. Both the analyses accurately take into account the steric interaction as a main driving force for the flip about the C11=C12 bond.

3.3. DFT ANALYSIS

The third optimization method used in our calculations is the density functional theory. Different from HF-based methods, DFT uses the electron density as a variable to calculate the molecular energy, including electron–electron interactions. Because the density is a function of spatial coordinates, the energy, is therefore, a density functional. Kohn and Sham [9] proved that there does exist an exact functional that can correctly predict these energies; however, it has never been found. There have been many functionals created which make a very good approximation. One of the most popular

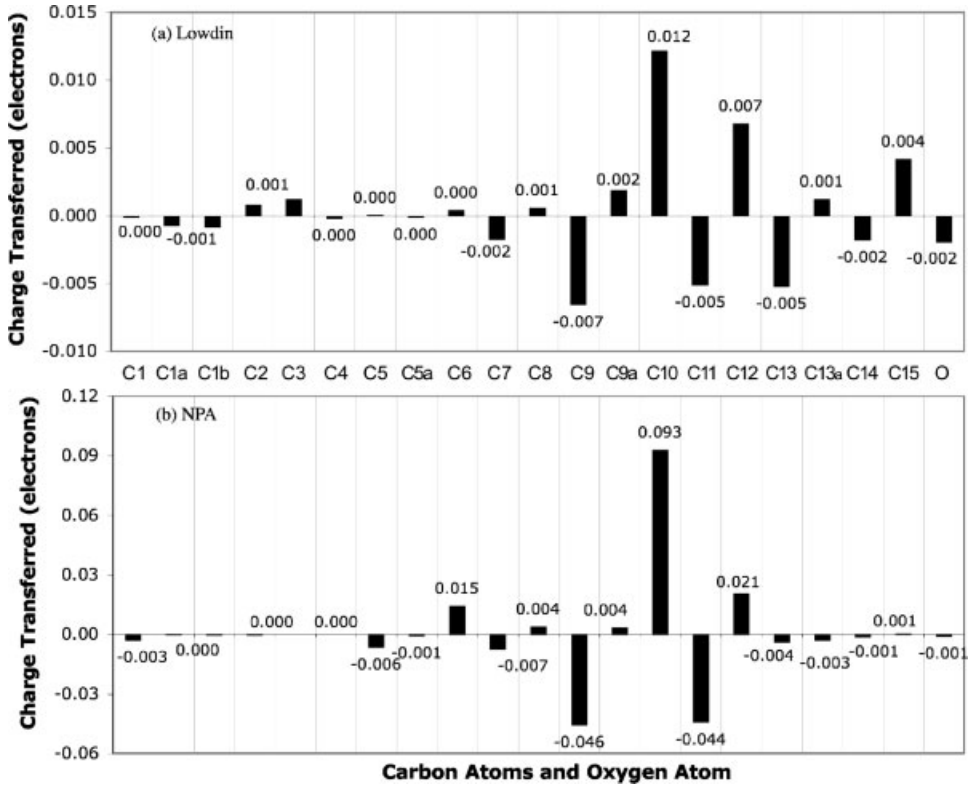

FIGURE 8. Charge transfer in rhodopsin calculated using the (a) Löwdin population analysis and (b) NPA with structures optimized by the DFT method.

is the B3LYP hybrid functional, which uses Becke's exchange functional in a linear combination with exact exchange energy from Hartree-Fock theory, as well as a correlation part from Lee, Yang, and Parr [15, 16]. After optimization of retinal with the DFT method, the energy gap between the 11-cis and all-trans configurations was calculated to be 0.218 eV, closest to the experimental value (0.206 eV [8, 11]) out of all the three methods.

When looking at the difference in structure of 11-cis and all-trans retinal after optimization by DFT, there were some similarities and differences to the HF method. In the case of DFT, the optimized geometry of 11-cis retinal had the tail positioned slightly forward, making it most likely for the dihedral flip to occur clockwise by 179 degrees; however, the definite direction of torsion is still unknown. As it did with the HF method, the carbon backbone of trans retinal settled into a planar configuration upon adjustment of the linear and dihedral bond angles in the isomerization region. A new result that the optimization by DFT brought is the many changes in bond lengths throughout the molecule. Along the carbon chain, all of the double bonds were shortened by ~2%, the largest being the C11=C12 bond which was shorter by 2.5% (0.034 Å) in the trans configuration than that of the cis bond length. In addition, all of the C–C single bonds were longer by ~1%, the largest being the C10–C11 bond which was elongated by 1.5% (0.021 Å). Lastly, all of the hydrogen bonds were shortened by 1% (≈.01 Å) in going from cis to trans. We can see if these differences have any effect on the charge distributions.

In comparison with results from the HF calculations, the five population analysis methods kept a similar resemblance, in a sense that they separated into Mulliken, NPA and Löwdin, and ESP groups. However, compatible with our previous conclusion, the Mulliken and ESP methods calculated with DFT were extremely different from that of previous ab initio methods, whereas the Löwdin analysis and NPA remained consistent. The latter two population analyses, as depicted in Figure 8, demonstrate nearly identical results to the charge redistribution calculations by the HF method. It shows that the orthogonalization of the basis set distributes the partial charge amongst the atoms in a way that produces the same data regardless of the quantum-chemical method used. This is the sign of a more robust population analysis. It also validates the

conclusions drawn about the charge redistribution in the retinal of Rh from the previous ab initio methods.

4. Conclusion

We have made a detailed quantum-chemical analysis of the charge distribution of the retinal chromophore of rhodopsin (Rh) and bacteriorhodopsin (BRh) using the RHF, MP2, and DFT methods with the 6-31++G** basis set. Although all three methods proved to have reliable results, MP2 is the most appropriate method for our calculations because it includes electron correlation effects which became apparent in our charge redistribution calculations. After comparison of five key population analysis methods, we conclude that both the Löwdin and natural population analyses are the most reliable for complex molecules, such as retinal. Notably, the NPA reveals important details of the proposed charge redistribution mechanism responsible for the isomerization of Rh when using MP2 optimized configurations. Calculation of the transition state of the reaction would provide further evidence for our hypothesis, however, based on spectroscopic data of the reaction path [4] and our comparison of charge distributions, we deduce that charge transfer occurs. We propose that upon excitation of the molecule, the induced electric field, as observed in [3], causes the charged particles in the molecule to react in the way that is observed by the MP2 NPA and Löwdin charge redistribution analyses. The negative charge that is gained by the hydrogens in the C13a methyl group causes a large repulsion from the H10 hydrogen attached to the C10 carbon. This steric interaction, as described by Lin et al. [2], is demonstrated in that way that C10 sends charge upward to the C9 and C11 atoms and is what drives 11-cis retinal to flip into the all-trans structure about the C11=C12 bond, also noted by the gain of charge by C11 from C10 and C12. The NPA charge redistribution analysis reflects this interpretation by including a large gain of negative charge by the H11 and H12 hydrogens, which are known for their role in the isomerization mechanism as the decoupled hoop-out-of-plane modes [14].

We conclude that charge redistribution in and around the isomerization region is the mechanism behind the dynamical changes of retinal in rhodopsin. We assert that MP2 is an appropriate quantum-chemical method for optimization calculations of large and complex molecules because of the manner in which it includes electron correlation effects. Lastly, we demonstrated the reliability of the Löwdin and natural population analyses in the calculation of charge distributions for large molecules.

ACKNOWLEDGEMENT

The authors are grateful to Wolfgang Domcke and Phil Bucksbaum for their valuable discussions.

References

1. Schoenlein, R. W.; Peteanu, L. A.; Mathies, R. A.; Shank, C. V. Science 1991, 254, 412.
2. Lin, S. W.; Groesbeek, M.; van der Hoef, I.; Verdegem, P.; Lugtenburg, J.; Mathies, R. A. J Phys Chem B 1998, 102, 2787.
3. Groma, G. I.; Hebling, J.; Kozma, I. Z.; Varo, G.; Hauer, J.; Kuhl, J.; Riedle, E. PNAS 2008, 105, 6888.
4. Kukura, P.; McCamant, D. W.; Yoon, S.; Wandschneider, D. B.; Mathies, R. A. Science 2005, 310, 1006.
5. Frisch, M. J.; Trucks, G. W.; Schlegel, H. B.; Scuseria, G. E.; Robb, M. A.; Cheeseman, J. R.; Montgomery, J. A., Jr.; Vreven, T.; Kudin, K. N.; Burant, J. C.; Millam, J. M.; Iyengar, S. S.; Tomasi, J.; Barone, V.; Mennucci, B.; Cossi, M.; Scalmani, G.; Rega, N.; Petersson, G. A.; Nakatsuji, H.; Hada, M.; Ehara, M.; Toyota, K.; Fukuda, R.; Hasegawa, J.; Ishida, M.; Nakajima, T.; Honda, Y.; Kitao, O.; Nakai, H.; Klene, M.; Li, X.; Knox, J. E.; Hratchian, H. P.; Cross, J. B.; Bakken, V.; Adamo, C.; Jaramillo, J.; Gomperts, R.; Stratmann, R. E.; Yazyev, O.; Austin, A. J.; Cammi, R.; Pomelli, C.; Ochterski, J. W.; Ayala, P. Y.; Morokuma, K.; Voth, G. A.; Salvador, P.; Dannenberg, J. J.; Zakrzewski, V. G.; Dapprich, S.; Daniels, A. D.; Strain, M. C.; Farkas, O.; Malick, D. K.; Rabuck, A. D.; Raghavachari, K.; Foresman, J. B.; Ortiz, J. V.; Cui, Q.; Baboul, A. G.; Clifford, S.; Cioslowski, J.; Stefanov, B. B.; Liu, G.; Liashenko, A.; Piskorz, P.; Komaromi, I.; Martin, R. L.; Fox, D. J.; Keith, T.; Al-Laham, M. A.; Peng, C. Y.; Nanayakkara, A.; Challacombe, M.; Gill, P. M. W.; Johnson, B.; Chen, W.; Wong, M. W.; Gonzalez, C.; Pople, J. A. Gaussian 03, Revision D.02; Gaussian, Inc.: Wallingford CT, 2004.
6. Martin, F.; Zipse, H. J Comput Chem 2004, 26, 97.
7. Prokhorenko, V. I.; Nagy, A. M.; Waschuk, S. A.; Brown, L. S.; Birge, R. R.; Miller, R. J. D. Science 2006, 313, 1257.
8. Birge, R. R. Biochim Biophys Acta 1990, 1016, 293.
9. Cramer, C. J. Essentials of Computational Chemistry; Wiley: New York, 2002.
10. Szabo, A.; Ostlund, N. S. Modern Quantum Chemistry; Dover: New York, 1996.
11. Bifone, A.; de Groot, H. J. M.; Buda, F. J Phys Chem B, 1997, 101, 2954.
12. Sigfridsson, E.; Ryde, U. J Comput Chem 1998, 19, 377.
13. Reed, A. E.; Weinstock, R. B.; Weinhold, F. J Chem Phys 1985, 83, 735.
14. Yan, E. C. Y.; Ganim, Z.; Kazmi, M. A.; Chang, B. S. W.; Sakmar, T. P.; Mathies, R. A. Biochemistry 2004, 43, 10867.
15. Becke, A. D. J Chem Phys 1993, 98, 5648.
16. Stephens, P. J.; Devlin, F. J.; Chabalowski, C. F.; Frisch, M. J. J Phys Chem 1994, 98, 11623.